THROUGH OPTIMIZATION OF A WINGED BOOSTER TRAJECTORY OF REUSABLE AEROSPACE SYSTEM AND PECULIARITIES OF ITS FLIGHT TRY-OUT

A.S. Filatyev*, O.V. Yanova*, N.N. Ryabukha**
*Central Aerohydrodynamic Institute (TsAGI)
** Gromov Flight Research Institute (FRI)

Keywords: through optimization, the maximum principle, through landing footprint, reusable winged booster, alternative concept

Abstract

The Pontryagin maximum principle serves the basis for through optimization of the reusable aerospace system (RASS) with recoverable winged booster (RWB) trajectory. This approach accounts for control and trajectory constraints throughout the RASS and RWB flight phases. Comparison is made of the RASS and RWB basic and alternative concepts, which differ in RWB landing site (the base airfield in the launch area against a recovery airfield available along the power-off re-entry path). 'Through' landing footprints are constructed with regard to both maneuverability of the RWB at autonomous reentry, and RASS maneuverability at launch. The RWB flight trials and transportation peculiarities are analyzed for the alternative RASS concept.

1 Introduction

The reusable aerospace system (RASS) [1] currently under development in the Khrunichev Space Center has primary reusable recoverable winged 1st stage boosters (RWB). Featuring a fixed-wing configuration, they enable an autonomous aircraft-type landing and serve intrinsically an unmanned aerial vehicle (UAV) equipped with the cruise propulsion and fuel tanks for the powered flight of the RASS insertion phase. On staging, the RWB re-enters the atmosphere and flies down to the landing site. According to the RASS basic concept [1], on staging the RWB makes an atmospheric turn towards the base airfield in the launch-site area. The air-breathing engines (ABE) start at an
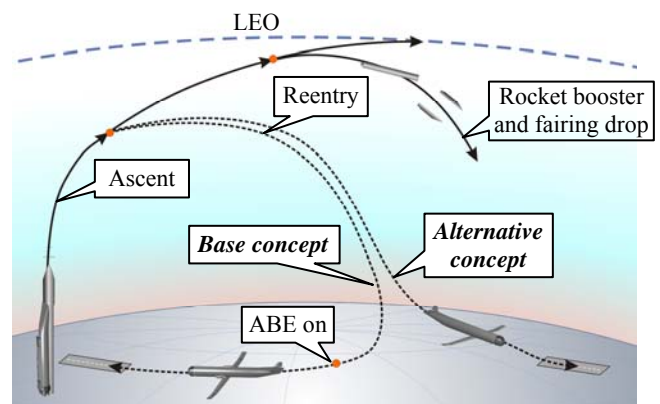

Fig. 1. The scheme of RASS branching trajectory

altitude of ~ 7-9 km to power the cruise flight (approximately 500 km) and the landing (Fig. 1). Thus stated in the basic concept, the ABE and relevant fuel have to be taken spaceward first idle in order to power only the final stage of flight, which makes the specific costs rise drastically, up to 300-400 \$/kg. The alternative concept [2] introduces a power-off RWB landing on a recovery airfield along the insertion path available at power-off atmospheric maneuvering after staging (Fig. 1).The RWB is further shipped by rail, sea, road or air to the base airfield (in the latter case the ABE can be mounted onto the RWB to enable its autonomous flight to the launch site)[2].

The alternative concept has a number of advantages over the basic concept, namely:

- reduction of the RWB weight due to elimination of the ABE and relevant fuel,
- reduction of the 1st stage RASS drag due to improved layout of the aerospace vehicle without the air breathers,

- reduction of aerothermodynamic heating at RWB re-entry in dense atmosphere as approach and landing on a recovery airfield along the insertion path require less roll angles than maneuvering towards the base airfield,
- no need to consider an insufficiently studied issue of ABE starting after the flight in negligible atmosphere with quasi-zero gravity and re-entry into the dense air with high aerothermodynamic loads.

As far as the reliability of the power-off landing is concerned, the experience gained from long flying practice and landings with shutdown engines (a compulsory routine of pilot training) along with analysis made in the framework of the Buran project, availability of the engines with a limited fuel range does not offer any considerable advantage over a power-off landing.

It is important to note that the alternative concept is feasible only for inland launch-sites, typical of Russia. A shortcoming until recently as the inland location has made vast impact areas economically unusable; it has turned an advantage due to availability of airfields for the RWB landings instead of drop areas. Moreover, there are few offshore strips allocated for the impact areas nowadays, and the seaside spaceports continuously lose their serviceability in this respect.

According to the Russian Federal Program for the Far East development, the transport infrastructure is to be elaborated in the region, which implies sufficiently low extra expenses and resources for equipping the RWB recovery airfields with landing and servicing equipment, yet making the RASS project more attractive in terms of investment due to a great diversification of infrastructure.

This paper presents comparison of the two RASS concepts in terms of the payload factor, reliability and safety. The through optimization of the RASS branching trajectories enables construction of the RWB through landing footprints (with regards to the RASS maneuverability at orbit insertion); this analysis involves an updated ASTER complex [3] based on indirect optimization method – the Pontryagin maximum principle [4].
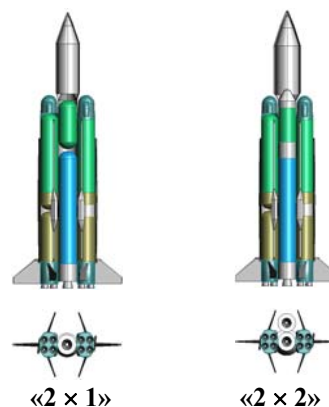

«2 × 1»   «2 × 2»
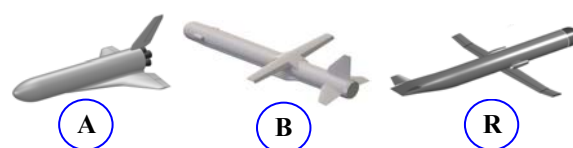
Fig. 2. RASS layouts

A   B   R

Fig. 3. RWB types

The flight testing routine and RWB transportation to the launch site are elaborated in respect of extensive practice of aircraft development and testing including the 'Buran' Space Vehicle program to ensure their reliability, cost-effectiveness, and minimum risks.

2 RASS description

The RASS [1] consists of a reusable first stage based on the RWB, an expendable second stage, consisting of a single or several central boosters (CB) and an upper stage booster (USB) with a payload. RASS family is based on a modular approach and provides injection of payloads weighing from ~20 to ~60 tons into low-Earth orbit (LEO) with the altitude of 200 km.

In this paper the study of two RASS layouts (see Fig.2) was carried out:
- the layout «2+1» consists of one CB and two RWB with rectangular wing (type B),
- the layout «2+2» consists of two CB and two RWB with delta wing (type A) or of type 'transformer' (type R).

The RWB types under consideration are described in Table 1 and shown in Fig.3. Types marked by '–' do not have ABE with its fuel in the launch configuration.

The main RASS parameters are given in Table 2.

Table 1: RWB types

Designation	ABE	Wing type	Recovery concept
A^+	+	Delta wing	back to the launch site airfield
A^-	–	(Buran-type)	landing on an alternative airfield
B^+	+	Rectangular tilting wing	back to the launch site airfield
B^-	–	(of RWB «Baikal» type)	landing on an alternative airfield
R	–	Unswept tilting wing with unfolding half wings ('transformer')	landing on an alternative airfield

Table 2. RASS parameters

Parameter	Relative value	
	Layout «2+1»	Layout «2+2»
Launching mass[*)]	1	1
RWB launching mass[**)] including:	2*0.3665	2*0.3210
– main engines fuel	2*0.3099	2*0.2796
– RWB staging part including:	2*0.0536	2*0.04144
- ABE mass	6×0.0043	6×0.002857
- ABE fuel	6×0.0066	6×0.003643
- dry mass	2×0.0209	2×0.02194
CB lunching mass including:	0.2344	2*0.1790
– main engines fuel	0.2066	2*0.1399
– payload fairing mass	0.0278	0.005714
– CB staging part including	0.0278	2*0.01610
– USB mass	0.0326	0.04008

[*)] the same for all RWB variants under consideration
[**)] corresponds to the launching mass of RWB A^+ in RASS layout «2+2» and to the launching mass of RWB B^+ in RASS layout «2+1»; relative masses of other RWB types under review are shown in Table 3

Table 3. RWB relative masses $\overline{m}_{WB}$

	RWB types				
	A^+	A^-	B^+	B^-	R
$\overline{m}_{WB}$	1	0.95595	0.86836	0.84248	0.97975

RWB R differs from A and B ones significantly in terms of design and application [5]:
- no ABE in the launch configuration,
- an unswept tilting wing with fold-out half wings; which aspect ratio is 1.3 times higher as compared to B^+ while the wing area is maintained,
- V-tail (45º swept) comes out of the wedge-shaped airframe fairing at free flight, its area is reduced $\sqrt{2}$ times as compared to B^+,
- main engines are closed with the heat shielding doors of the fairing after the RWB separation (it is supposed that their mass equals that of the fairing on RWB B^+),

- to fulfill the recovery, the RWB makes a 180º turn with its wedged-shaped fairing backwards simultaneously with the wing tilt, approximately at maximum altitude.

Main engines mounted on the RWB run on liquid methane and oxygen (liquefied natural gas). The main engine of CB uses oxy-hydrogen fuel. Data on main engines employed for the calculations are shown in Table 4.

Table 4. RASS main engines data

Characteristic	RWB A and R	RWB B	CB
Number of engines per booster	4	4	1
Engine type	RD-191	RD-0162	RD-0120
Effective[*)] thrust in vacuum, t	212	225	190/147
Specific impulse in vacuum, s	337	356	455
Specific impulse at sea level, s	309.5	321.2	352

[*)] in view of the angle of engine setting

The aerodynamic lift C_L and drag C_D coefficients are given as:

$$C_L = C_{L\alpha} \cdot \alpha, \;\; C_D = C_{D0} + A_D C_L^2,$$

where α is an angle of attack, coefficients $C_{L\alpha}$, C_{D0}, A_D are functions of the Mach number (see Tables 5-7). Aerodynamic characteristics of RASS with RWB R are adjusted compared with [2]. The aerodynamic coefficients of the RASS 2nd stage are defined as: $C_{D0} = 0.58$, $A_D = 0.125$, $C_{L\alpha} = 0.139$ 1/deg through the all velocity range. The aerodynamic characteristics of RASS with RWB B and RWB B in autonomous flight are supposed to not depend on the presence of ABE.

The RASS insertion phase and RWB reentry are interrelated. So these two trajectory legs must be analyzed simultaneously in order to obtain objective data on the optimal trajectories and vehicle parameters effect on the problem functional. This makes us consider and optimize the RASS branching trajectories [6].

Table 5: RASS aerodynamic characteristics

	Layout «2+1»			Layout «2+2»								
	RWB B			**RWB A$^+$**			**RWB A$^-$**			**RWB R**		
M	C_{D0}	A_D	$C_{L\alpha}$, 1/deg	C_{D0}	A_D	$C_{L\alpha}$, 1/deg	C_{D0}	A_D	$C_{L\alpha}$, 1/deg	C_{D0}	A_D	$C_{L\alpha}$, 1/deg
0	0.442	0.0724	0.29	1.244	0.0292	0.500	1.2444	0.0292	0.5	0.34	0.0733	0.275
0.4	0.442	0.0768	0.302	1.249	0.0296	0.530	1.2485	0.0296	0.53	0.35	0.0737	0.272
0.6	0.571	0.0766	0.317	1.294	0.0302	0.598	1.2937	0.0302	0.599	0.37	0.0730	0.269
0.8	1.219	0.0602	0.346	1.784	0.0287	0.700	1.784	0.0287	0.7	0.43	0.0634	0.268
1	2.291	0.0556	0.3870	3.656	0.0239	0.750	3.091	0.0239	0.75	0.55	0.0581	0.272
1.2	2.942	0.0675	0.3201	4.387	0.0246	0.718	3.6	0.0246	0.718	0.62	0.0578	0.280
1.5	3.019	0.0809	0.2628	4.145	0.0276	0.668	3.5	0.0276	0.668	0.61	0.0591	0.299
2	2.873	0.093	0.2237	3.681	0.0321	0.596	3.2	0.0321	0.596	0.53	0.0615	0.331
3	2.537	0.109	0.175	3.051	0.0435	0.490	2.7	0.0435	0.49	0.45	0.0700	0.351
4	2.251	0.1335	0.151	2.616	0.0621	0.405	2.33	0.0621	0.405	0.385	0.0809	0.345
5	2.070	0.1661	0.1359	2.396	0.0830	0.340	2.1	0.0830	0.34	0.33	0.0957	0.315
7	1.801	0.23	0.11	2.180	0.1126	0.272	1.855	0.1126	0.272	0.25	0.1184	0.260

Table 6. Aerodynamic characteristics of RWB A$^+$ and A$^-$

	A$^+$			**A$^-$**		
M	C_{D0}	A_D	$C_{L\alpha}$, 1/deg	C_{D0}	A_D	$C_{L\alpha}$, 1/deg
0	0.0518	0.159	0.0543	0.0518	0.159	0.0543
0.26	0.0518	0.159	0.0543	0.0518	0.159	0.0543
0.6	0.0548	0.205	0.0601	0.0548	0.205	0.0601
0.8	0.0631	0.245	0.0724	0.0631	0.245	0.0724
0.9	0.0942	0.280	0.0707	0.0942	0.280	0.0707
1	0.1393	0.261	0.0785	0.1300	0.261	0.0785
1.2	0.1556	0.317	0.0625	0.1380	0.317	0.0625
1.5	0.1476	0.384	0.0504	0.1300	0.384	0.0504
2	0.1347	0.498	0.0385	0.1150	0.498	0.0385
3	0.1200	0.680	0.0268	0.1000	0.680	0.0268
4	0.1082	0.859	0.0209	0.0905	0.859	0.0209
5	0.1036	1.018	0.0179	0.0850	1.018	0.0179
7	0.1033	1.075	0.0168	0.0835	1.075	0.0168

Table 7. Aerodynamic characteristics of RWB B and R

	B			**R**		
M	C_{D0}	A_D	$C_{L\alpha}$, 1/deg	C_{D0}	A_D	$C_{L\alpha}$, 1/deg
0	0.0635	0.044	0.2222	0.0444	0.034	0.2380
0.29	0.0635	0.044	0.2222	0.0444	0.034	0.2380
0.4	0.0637	0.047	0.2231	0.0449	0.036	0.2382
0.61	0.0925	0.075	0.2467	0.0673	0.059	0.2640
0.78	0.1375	0.114	0.2200	0.3448	0.100	0.2564
1	0.4000	0.100	0.2564	0.3560	0.229	0.0771
1.67	0.3922	0.229	0.0771	0.3450	0.405	0.0475
2.5	0.3654	0.405	0.0475	0.3378	0.528	0.0368
4	0.3462	0.528	0.0368	0.3311	0.614	0.0264
7	0.3364	0.614	0.0264	0.0444	0.622	0.2380

3 Through optimization of RASS branching trajectories

The RASS branching trajectory comprises the main branch, i.e. the powered insertion and side branches, i.e. power-off reentry paths of the reusable winged booster and the 2nd stage separating parts (SP) (booster and fairing doors) (refer to Fig. 1). The powered insertion in its turn comprises the RASS 1st and 2nd stage flight phases. Parameters of the trajectory late in the powered phase determine drop of the SP right in

the antipode of the launching point. With the separation of the 2nd stage SP, the upper stage takes the payload to the target orbit. The side branch corresponding to the RWB return trajectory is included into the optimization process. The effect of the 2nd stage SP trajectory on the RASS trajectory is taken into account by introducing the flight profile in the staging point (including mass variation).

3.1 Problem statement

The motion of RASS parts is described by a normal system of ordinary differential equations in the initial coordinate system [7]:

$$\frac{d\mathbf{x}}{dt} = \mathbf{f}(\mathbf{x}, \mathbf{u}, t),$$

$$\mathbf{f} = \left\{ \mathbf{v}, \frac{\mathbf{T} + \mathbf{A}}{m} + \mathbf{g} + \mathbf{\Omega}, -\mu \right\}^{\mathrm{T}}, \qquad (1)$$

where $\mathbf{x} = \{\mathbf{r}, \mathbf{v}, m\}^{\mathrm{T}} \in \mathbf{X}$ is the state vector, $\mathbf{r}$ is the radius vector, $\mathbf{v} = v\mathbf{e}_v$ is the velocity vector, m is the mass, $\mathbf{f}$ is the right member vector, $\mathbf{u} \in \mathbf{U}$ is the control vector, $\mathbf{g}$ is the gravity acceleration, $\mathbf{\Omega} = (\mathbf{\omega} \times \mathbf{R} + 2\mathbf{v}) \times \mathbf{\omega}$ is the acceleration vector due to noninertial coordinate system (initial launch-site coordinate system), $\mathbf{\omega}$ - spin vector of the Earth daily revolution, $\mathbf{R} = R\mathbf{e}_R = \mathbf{r} + \mathbf{R}_0$, $\mathbf{R}_0$ is the radius vector of the Earth center to the reference point (the starting point), μ is the specific fuel consumption, $\mathbf{T} = T \cdot \mathbf{e}_{\mathrm{T}}$ is the thrust vector, $\mathbf{e}_{\mathrm{T}}$ is the unit thrust vector, $\mathbf{A}(R, \mathbf{v}, \mathbf{e}_\tau)$ − aerodynamic force,

$\mathbf{e}_\tau$ is the unit vector along the longitudinal vehicle axis, $t \in [t_i, t_f]$ is the time,

Slip is assumed to be absent and the thrust vector is directed along the longitudinal vehicle axis:

$$\mathbf{e}_T = \mathbf{e}_\tau . \qquad (2)$$

With regard to (1), (2) control vector components are

$$\mathbf{u} = (\mathbf{e}_\tau, T). \qquad (3)$$

At the RWB return trajectory constraints on the angle of attack α, bank angle σ, allowable normal g-load factor n_y, and dynamic pressure q are imposed:

$$\begin{aligned} |\alpha| &\le \alpha_{\max}, \ |\sigma| \le \sigma_{\max}, \\ n_y &\le n_{y\,adm}, \ q \le q_{adm}. \end{aligned} \qquad (4)$$

At the initial time moment t_i the state vector is assumed to be either fixed completely or with a free orientation of the velocity vector while the other state vector components are fixed (in this case the orientation of the initial velocity vector is the optimal one).

At the end of active leg there are given flight conditions on a single-turn orbit with an apogee

$$R(t_f) = R_f, \qquad (5)$$

which provide the fall of the 2nd stage SP in an antipodal point of the Earth. The flight of USB in the transfer orbit beyond the notional boundary of the atmosphere (where the aerodynamic forces can be neglected) is approximately replaced by the Kepler arc. An apogee of the transfer orbit coincides with the radius of the target circular one and its perigee coincides with an apogee of the single-turn orbit (5). Active legs on the transfer orbit are replaced by velocity impulses in apogees of single-turn (5) and transfer orbits.

The following optimization problems are considered.

Problem 1. With the RWB landing site assigned (the geographic latitude φ_{sf} and longitude λ_{sf}), the problem is to find an optimal control over the spatial orientation at RASS ascent and RWB reentry so that the inserted mass be maximized with constraints on the control and trajectories:

$$\Phi_1 \equiv m(t_f) \Rightarrow \max_{\mathbf{u}} \Big|_{(\varphi_{sf}, \lambda_{sf}) - fix} . \qquad (6)$$

(The subscript «s» corresponds to a side branch.)
Problem 2. With the inserted mass specified, the problem is to find an optimal control over the spatial orientation at RASS ascent and RWB reentry so that the RWB gliding range ΔL in the chosen direction $\mathbf{e}_L$ in a local horizontal plane be maximized:

$$\Phi_2 \equiv \Delta L_{sf}(\mathbf{e}_L) \Rightarrow \max_{\mathbf{u}} \Big|_{m_f - fix} . \qquad (7)$$

The first problem brings us to the RASS limit payload capacity providing the RWB landing to an assigned airfield.

The second problem enables to calculate the boundary of «through» landing footprints (TLF) for the assigned RASS inserted masses by rotating the direction vector $\mathbf{e}_L$ in a circle.

A landing footprint is meant the limit region of Earth surface (or a spherical surface at the altitude of an aiming keypoint at automatic landing) which RWB can reach in autonomous passive flight. The term 'through' is introduced to underline that this landing footprint depends both on the extreme RWB maneuverability in the autonomous flight and on optimum trajectory of the RASS powered insertion.

A similar problem statement has been considered earlier in work [8] for analytical synthesis of critical disturbances on RASS trajectories.

3.2 RWB control structure

RWB control structure is defined in accordance with an approximately optimal law of changing the angles of attack and roll [9], [10]:

$$\alpha_{opt} = \begin{cases} \alpha_{\max}, \ \psi \ge \pi/2, \\ \alpha_{K\max}, \ \psi < \pi/2, \end{cases} \qquad (8)$$
$$\sigma_{opt} = \begin{cases} \sigma_{\max}, \ \psi \ge \sigma_{\max}, \\ \psi, \ \psi < \sigma_{\max}, \end{cases}$$

where $\alpha_{K\max}(\mathbf{x})$ is the angle of attack corresponding to the maximum RWB lift-drag ratio $(L/D)_{\max}$, $\alpha_{\max}$ is the maximum permissible angle of attack with regard to the imposed limitations (4), ψ is the azimuthal angle between projections to a local horizontal plane of the velocity vector $\mathbf{v}$ and the vector $\mathbf{e}_L$:

$$\psi = \arccos(\mathbf{e}_v, \mathbf{e}_L). \tag{9}$$

In accordance with (6), (7) the RWB orientation control vector $\mathbf{e}_\tau$ is

$$\begin{aligned}
&\mathbf{e}_\tau = a_0\mathbf{e}_\tau + b_0\mathbf{e}_v + c_0(\mathbf{e}_v \times \mathbf{e}_R), \\
&a_0 = \cos\alpha_{opt} - b_0\sin\sigma_{opt}, \\
&b_0 = \frac{\sin\alpha_{opt}\cdot\cos\sigma_{opt}}{\cos\gamma}, \\
&c_0 = \frac{\sin\alpha_{opt}\cdot\sin\sigma_{opt}}{\cos\gamma},
\end{aligned} \tag{10}$$

where $\gamma = \arccos(\mathbf{e}_R \times \mathbf{e}_v)$ is the trajectory angle.

3.3 Optimality conditions

On the base of the Pontriagin maximum principle [4] the optimal control is defined from the condition

$$\mathbf{u}_{opt} = \arg\max_{\mathbf{u}(t)\subset\mathbf{U}}\mathcal{H}, \tag{11}$$

where $\mathcal{H} = \mathbf{\Psi}^T\mathbf{f}$ is the Hamiltonian, $\mathbf{\Psi} = \{\mathbf{P}, \mathbf{S}, P_m\}^T$ is the conjugate vector, corresponding to the state vector $\mathbf{x}$. The vector $\mathbf{\Psi}$ satisfies the equation:

$$\dot{\mathbf{\Psi}} = -\left(\frac{\partial\mathcal{H}}{\partial\mathbf{x}}\right)^T = -\left(\frac{\partial\mathbf{f}}{\partial\mathbf{x}}\right)^T\mathbf{\Psi} \tag{12}$$

with boundary (transversality) conditions derived in [6]. In particular, in branching points the conditions of the state vectors' continuity result in the following conditions of the jump of conjugate variables (transversality conditions):

$$\begin{aligned}
&\mathbf{\Psi}^+ = \mathbf{\Psi}^- - \mathbf{\Psi}_s - \lambda\left(\frac{\partial Q_0}{\partial\mathbf{r}}\right)^T, \\
&\mathcal{H}^+ = \mathcal{H}^- - \mathcal{H}_s,
\end{aligned} \tag{13}$$

where Q_0 is the condition of implicit definition of the branching moment τ_0: $Q_0(\mathbf{x})\big|_{\tau_0} = 0$.

Transversality conditions at the right end of RWB return trajectory (at the time moment t_{sf}) differ in considered problems (6), (7).

In Problem 1 taking into account the specified point of RWB landing

$$\mathbf{Q}_f(\mathbf{x}(t_{sf})) = \mathbf{r}(t_{sf}) - \mathbf{r}_{sf} = 0 \tag{14}$$

transversality conditions are [11]:

$$t = t_{sf} : \begin{cases} \mathbf{P}_{sf} = \mathrm{var}, \\ \mathbf{S}_{sf} = 0, \\ P_{m\,sf} = 0, \\ \mathcal{H}_{sf} = (\mathbf{P}^T\mathbf{v})_{sf} = 0, \end{cases} \tag{15}$$

where the time moment t_{sf} is defined implicitly by achieving altitude h_{sf} specified in (14):

$$t_{sf} : Q_h = h(t_{sf}) - h_{sf} = 0. \tag{16}$$

In Problem 2 at the right end of RWB return trajectory transversality conditions are [8]:

$$\mathbf{\Psi}_{sf}^L = \mathbf{\Psi}_s^L(t_{sf}) = \nabla(\Delta L) - \frac{\nabla(\Delta L)\cdot\dot{\mathbf{x}}(t_{sf})}{\nabla Q_h\cdot\dot{\mathbf{x}}(t_{sf})}\cdot\nabla Q_h, \tag{17}$$

The superscript $(\;)^L$ in (17) emphasizes the dependency of the conjugate vector on $\mathbf{e}_L$.

From (17) in view of (16):

$$\begin{aligned}
&\mathbf{P}_{sf}^L = \mathbf{e}_L - \frac{\mathbf{e}_L^T\mathbf{e}_v}{\mathbf{e}_{r_0}^T\mathbf{e}_v}\cdot\mathbf{e}_{r_0}, \\
&\mathbf{S}_{sf}^L = 0, \; P_{msf}^L = 0,
\end{aligned} \tag{18}$$

where $\mathbf{e}_{r_0}$ is the unit vector from the center of the Earth to the nominal RWB landing point, obtained from Problem 1 solving.

Transversality conditions at the right end of the main branch (at the time moment t_f) are also differ: in Problem 1 $P_m(t_f) = 1$, in Problem 2 $P_m(t_f)$ is not specified.

3.4 Boundary value problem peculiarities

The application of the Pontryagin maximum principle makes it possible to reduce the original problem of finding the optimal control in the functional space to the solution of the boundary value problem (BVP) for systems of ordinary differential equations (1), (12). The number of variable parameters of such BVP does not exceed the dimension of the state vector on the main branch n [12]. In the case of branching trajectories, each side branch increases the state space dimension by n_s (the dimension of the state vector on the side branch, which can not coincide with dimensions of state vectors on other branches), while the BVP dimension increases by n_s at most [3]. Thus, in the case of optimization of a trajectory with one side branch the BVP dimension does not exceed $n + n_s$.

At the same time, in some cases the increase of the BVP dimension with a side branch can be restricted by 1 or 2. The reduction of the BVP is achieved by projecting the boundary conditions (all or some of them) from the right ends of the side branches to the branching point. In particular this is possible when the control at the side branch is determined. In this case the control is the function of the state vector and time and does not contain conjugate variables. Then the solution of a vector linear differential equation (12) on a side branch can be represented as [3]:

$$\Psi(\tau_0) = \mathbf{A_x}^{-1}(\mathbf{x}) \cdot \Psi_{sf}, \qquad (19)$$

where $\mathbf{A_x}(\mathbf{x})$ is the transitional matrix obtained as a result of one-time solution of the Cauchy problem for the state set of equations (1).

The solution of the system (1) can be also obtained by a single iteration of a Newton method.

4 Numerical results

The numerical solutions of problems stated are realized in the automated program complex ASTER [3], [12] of the through optimization of branching trajectories. The automation of the multipoint BVP solution is provided using the modified Newton method, the solution

parameter continuation method in combination with the principle of local extremal selection, the vast database of the solutions obtained etc. [7], [8].

4.1 Optimal branching trajectories

As a result of Problem 1 solving the maximal inserted masses m_f, optimal trajectories and control programs are obtained for all RASS layouts and RWB types considered (Table 8).

Table 8. RASS maximal masses inserted into the target circular orbits (see Table 9)

	RASS layouts and RWB types				
	«2+1»		«2+2»		
	B^+	B^-	A^+	A^-	R
$\overline{m}_f$	1	1.0803	1	1.1015	1.2232

Table 9. Parameters of target orbits

	RASS layouts	
	«2+1»	«2+2»
Altitude h_{orb}, km	200	200
Inclination i_{orb}, deg	51.8454	51.7

The airfields location was supposed to be optimal for RWB with no ABE (A^-, B^- and R types), while RWB with ABE (A^+ and B^+ variants) are assigned to land in the launch site area. The masses of RWB considered see in Table 3. The fuel mass required for cruise flight to the launch site (constituent to A^+ and B^+ RWB masses) was estimated by using the Breguet formula [13]. On the RWB return trajectories constraints (3) were taken into account with

$$\alpha_{\max} = 50°, \ \sigma_{\max} = 65°,$$
$$n_{y\,adm} = 4, \ q_{adm} = 3000 \, kgs/m^2. \qquad (20)$$

As seen from Table 8 the relative advantage of maximal inserted mass within the alternative concept as compared with basic one is:

$$\Delta \overline{m}_f = \begin{cases} 0.1015 \text{ for RASS with WB A,} \\ 0.0803 \text{ for RASS with WB B.} \end{cases} \qquad (21)$$

The contribution into inserted mass advantage (21) of different factors (problem parameters) can be evaluated using the Bliss formula [14], connecting in each trajectory point variations of right parts of motion equations (1)
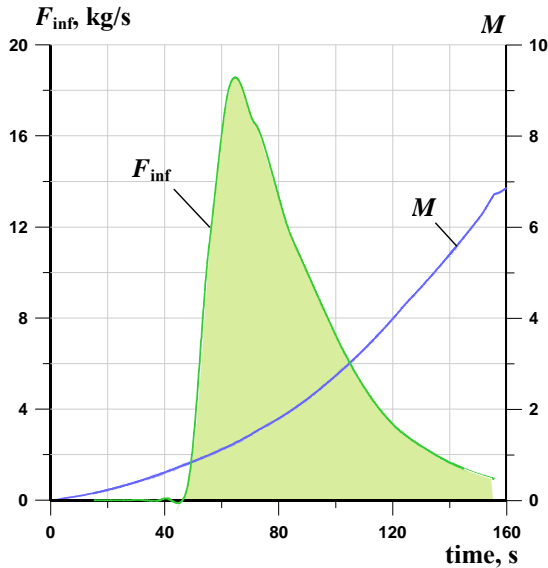
Fig. 4. F_{inf} and Mach number histories on the RASS injection trajectory with RWB A$^+$

$\Delta \mathbf{f}$ with the functional change through the vector Ψ of conjugate variables:

$$\Delta m_f = \int_{t_i}^{t_f} (\Psi, \Delta \mathbf{f}) dt . \qquad (22)$$

Lets evaluate the contribution into Δm_f defined by improvement of RASS aerodynamic characteristics at the expense of ABE elimination. The elimination of ABE results in a change of RASS mass and aerodynamic characteristics. Denote the corresponding changes of the system (1) right sides as $\Delta \mathbf{f}_m$ и $\Delta \mathbf{f}_A$:

$$\Delta \mathbf{f} = \Delta \mathbf{f}_m + \Delta \mathbf{f}_A . \qquad (23)$$

The vector $\Delta \mathbf{f}_A$ in each time moment is calculated with the replacement of aerodynamic parameters of RASS with ABE by parameters of RASS without ABE:

$$\Delta \mathbf{f}_A = \left\{ 0, \frac{1}{m} (\mathbf{A}_- - \mathbf{A}_+), 0 \right\}^T , \qquad (24)$$

where $\mathbf{A}_-$ и $\mathbf{A}_+$ are corresponding vectors of aerodynamic forces without and with ABE.

The integration element

$$F_{\text{inf}} = (\Psi, \Delta \mathbf{f}_A) \qquad (25)$$

is the specific sensitive function of the functional to a change of an aerodynamic forces at the moment. The square of the shaded region under the curve $F_{\text{inf}}(t)$ (the time integral)

$$\Delta m_{fA} = \int_{t_i}^{t_f} (\Psi, \Delta \mathbf{f}_A) dt \qquad (26)$$

determines the increment of inserted mass due to improvement of RASS aerodynamic characteristics by ABE eliminating. The maximum influence of aerodynamic parameters change is seen (Fig.4) to be in the transonic velocity range.

In the case of ABE elimination for RASS with RWB A the relation (26) gives us

$$\Delta \overline{m}_{fA} = 0.01624 , \qquad (27)$$

that equals 16% from the overall mass advantage (21) at the expense of abandonment of ABE mounting on the RWB of A-type.

In the whole the through optimization of the branching atmospheric ascent trajectories causes the gain of at least 5-8% of the payload mass in comparison with traditional gravitational-turn control program of RASS 1st stage [15].

4.2 Landing footprints

TLF of RWB without ABE are calculated by solving a series of through optimization problems for various directions of $\mathbf{e}_L$ in a circular range. In this case the $\mathbf{e}_L$ rotation angle on a local horizontal plane is the homotopy parameter of the solution continuation method.

Nominal (without random disturbances) TLF for the B$^-$-type RWB at RASS payload injection into orbits with 51.8454°, 72°, and 108° inclinations are shown in Fig. 5 in case of the maximal inserted mass of RASS ($\Delta \overline{m}_f = 0$), and extended due to optimal deformation of the insertion trajectory main branch, leading to some decrease of the inserted mass ($\Delta \overline{m}_f \leq 10\%$). Symbol "plane" shows available federal airfields which admissible for RWB landing. The green color symbols mark 1-st rate

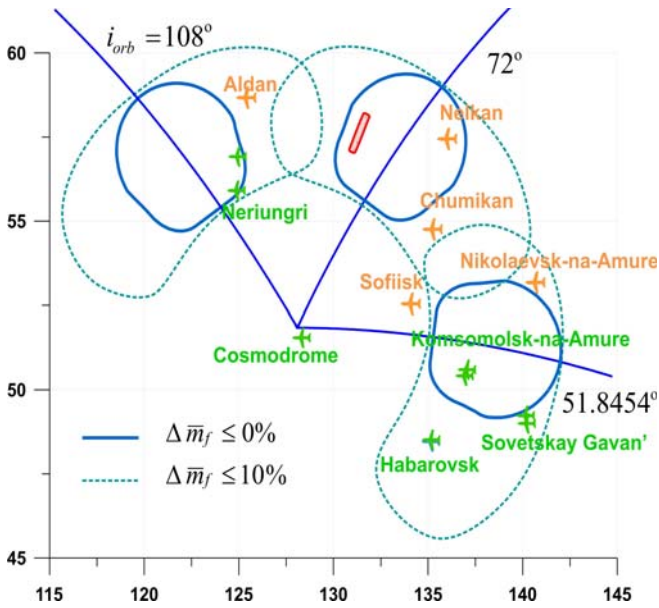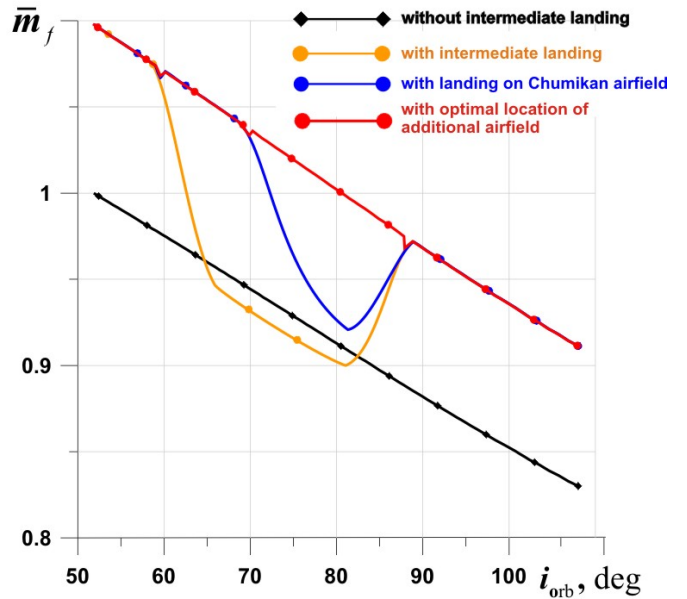Fig. 5. Through landing footprints of RWB A^-

Fig.6. The relative inserted mass $\overline{m}_f$ of RASS with RWB of B-type in dependence on the orbit inclination i_{orb} for the basic and alternative concepts

airfields, the orange color ones mark 2-nd rate airfields.

It is seen from Fig. 5 in case of injection into orbits with inclinations within a range of:

$$i_{op\delta} \in [51.8454°, 58.6°] \text{ and } i_{op\delta} \in [88.9°, 108°] \quad (28)$$

the requirement of RWB landing to the existing airfields (in the alternative concept) does not lead to any loss of the inserted mass.

Injection into orbits with inclinations within a range of:

$$i_{orb} \in [51.8454°, 61°] \text{ and } i_{orb} \in [77°, 108°] \quad (29)$$

can be fulfilled with no more than 10% loss of payload, which does not differ from the mass taken into the orbit by RASS with RWB A^+ and B^+ (with ABE) recovering to the launch site after staging (see Table 8). In case of the injection into orbits with inclinations (28), (29) the RWB B^- can land on 1st rate runways in Komsomolsk-on-Amur and Neryungri airfields.

A range of orbit inclinations, which do not correspond to any airfields available for RWB landing ('dead zone'), is about 15° from the considered range of 57°.

Fig. 6 shows the dependences of the relative inserted mass of RASS with RWB B on the target orbit inclination in the range of

$$i_{op\delta} \in [51.8454°, 108°] \quad (30)$$

for the basic and alternative concepts.

It is seen that in case of orbit inclinations (28) the realization of the alternative concept gives a gain of 10% of the inserted mass as compared with the basic concept. In case of injection into orbits with inclinations $i_{op\delta} \in (58.6, 88.9)°$ with RWB B^- landing on the Chumikan airfield the inserted mass losses are reduced to 0÷8%. And in case of optimal location of an additional airfield for the intermediate RWB B landing in the region with the center coordinates $(\varphi, \lambda) = (57.5°, 131.3°)$ (see Fig. 5) the mass of alternative layout of RASS inserted into orbits (30) exceeds the mass, inserted in accordance with the basic concept, more than 8.5%.

Similar calculations were done for RWB of A-type and R-type ('transformer') as part of RASS layout «2+2». Fig. 7 presents TLF for the RWB R, which has the maximum lift-to-drag ratio among the RWB types under consideration within a subsonic velocities range (see section 23). obtained for the RASS injection into orbits with the inclinations

$$i_{orb} \in [51.7°, 108°]. \quad (31)$$

As seen in Fig.7 better aerodynamic parameters of the RWB R enable to increase

TLF and practically nullify the 'dead zone' in the orbit inclination range (31). In this case the total range of orbit inclinations is available using only two airfields for RWB landing.

Injection into orbits with inclinations

$$i_{orb} \in \left[51.7°, 61.9°\right] \text{ and } i_{orb} \in \left[82°, 108°\right] \quad (32)$$

provides the maximal inserted mass. The relative gain of the inserted mass compared with RWB A$^+$ is

$$\Delta \overline{m}_f = 0.2232. \quad (33)$$

In case of target orbit inclinations in the range of

$$i_{orb} \in (61.85°, 82°) \quad (34)$$

the inserted mass decreases not more than 7% and with regard the basic concept is

$$\overline{m}_f = 1.2232 * 0.93 = 1.1346. \quad (35)$$

Thus the realization of the alternative concept of RASS injection with RWB of R-type enables to launch into orbits with inclinations in the range (31) 13% of inserted mass more than within the basic concept.

5 Peculiarities of RWB flight trials and transportation

Along with optimization of the RWB configuration and parameters defining its RASS-level object function, there is a good reason to seek intelligent solution to a number of typical satellite problems. Among these are first stages of RWB flight tests and transportation for example from an intermediate airfield (in the alternative concept) to a space port.

Both the USA and USSR initially employed similar concepts to find solution to this problem: with the specialized aircraft created by severe modernization of serial transport airplanes. In USA the Boeing-747 was extensively modified to become the Shuttle Carrier Aircraft (SCA). In USSR the 3M bomber was upgraded into the VM-T Atlant. The full cost of the development and test flights of the shuttle-carriers made up a substantial
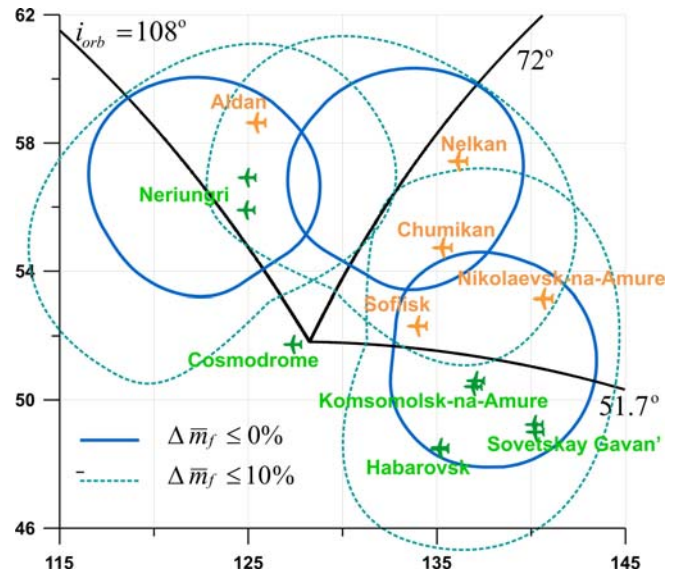

Fig. 7. Through landing footprints of RWB R

stake of the RASS overall project costs, while the operation and maintenance appeared troublesome (e.g. due to their wind sensitivity at takeoff and landing). So the experience thus gained has driven us to a conclusion that it is desirable to find a more cost-effective technology for the RASS configuration being considered [1].

A pretty conventional scope, flight tests are not easy to modify as any such modification is fraught with grave consequences, the more deviations from the established procedure the higher risks and eventually, higher expenditures. The basic RWB concept implied first flights tests with a release of the unmanned test item from the carrier. This variant offers the following peculiar features:

- a dedicated shuttle-carrier is needed;
- a remote launch site is needed for the flight tests;
- poor recoverability of the test item in case of emergency.

All the above considered, alternatively, the RWB flight tests are proposed to follow the well-elaborated procedures of the first stages testing of twin-engine aircraft. For this purpose the RWB main engine bay accommodates a standard two-seat pilot cockpit with ejection seats rather than liquid propellant system. The Su-34 cockpit appears to have the best geometry to match the structural shape of the RWB propulsion bay, yet other present-day Russian

fixed-wings can offer their cockpits as well with the Yak-130, Su-30, or MiG-29 among them. This concept features the following peculiarities of the WG transportation and flight testing:

- a two-seat cockpit module available for the winged booster must be accommodated in the cruise propulsion bay, including the RWB avionics interface with the cockpit indicators and controls. The standard heat-shielding fairing door must be replaced with the cockpit door;
- initial flight testing can be carried out in Moscow Region;
- flight safety is no worse than that typical of twin-engine aircraft flight testing.

The unmanned winged booster therefore for the flight testing transforms into a man-carrying aircraft to be developed, elaborated and operated according to the valid aviation regulatory system insofar as prototype aircraft are concerned. Moreover the tight standards established for the civil airliners need not be considered.

Removal of the aircraft engines from the RWB launch configuration (in compliance with alternative RWB re-entry concept) to a great extent predefines rational aircraft configurations for these engines. Among the range of Russian engines available at present, the well-elaborated and cost-effective D-30KP-2 (used in the IL-76 airlifters and are in world request) is suggested for the first flight testing stages, while the joint Russian - French SaM146 powerjet is proposed for the operational configuration. Table 10 gives principal performance of these two engines.

Table 10. Aircraft engine performance

Performance	D-30KP-2	SaM146
Thrust, kgf	12000	7200-7940
Specific fuel consumption at cruise kg/(kgf*hrs)	0.705	0.629
Mass, kg	2985	1700

With the RWB takeoff weight of approximately 50 tons (the alternative concept), the takeoff thrust-to-weight ratio of the aircraft equipped with the D-30KP-2 is of the order of 0.48. Such thrust-to-weight ratio appears excessive for the RWB operation, however makes sense for the initial stage of flight testing

as firstly, it extends the available range of altitude-speed performance (H≈12÷15km, M≈0.9), and secondly, improves flight safety margin (enables safe takeoff with one engine failed).

The takeoff thrust-to-weight ratio does not exceed 0.3 with the SaM146 powerjets, which falls in the range typical of the transport aircraft.

Both the basic and alternative concepts imply automatic unmanned flying to the space port, yet according to the alternative concept the engines start on the ground in the en-route aerodrome, rather than in the air. This serves the main factor to add to flight safety and reliability as compared to the basic concept.

Production flight tests and RWB transportation from the production plant to operational location can be carried out man-controlled with the SaM146 powerjets. This makes the winged booster no different from other aircraft both technically, and in legal aspect.

The basic concept involves substantial resource to carry the super heavy airlifter with the winged booster. Even rough estimations show that only the fuel costs to transport this structure with an overall takeoff weight of approximately 330 ÷ 350 tons and a landing weight around 250 tons will be 5 ÷ 7 times over the alternative concept fuel cost. Accounting for other direct and indirect costs to support the development and operation of the unique air transport system makes the estimate even worse. With the stated governmental policy towards the development of aerospace production centers in close proximity to the space ports, the purpose of such transport infrastructure is defeated. In fact, industrial localization of consumable daughter stage production in the cosmodrome area cracks the problem of regular hoist transportation of the winged boosters with no similar cargos in sight. The substantial funds attributed to the development of a dedicated air transport system with a super airlifter in the core along with the basic concept are thus unreasonable expenses. The alternative concept however offers an order of magnitude less costs to support the initial flight testing, RWB spaceport transportation, etc.

6 Conclusions

Analysis of the RASS basic [1] and alternative [2] concepts for various recoverable winged boosters (RWB) has shown effectiveness of such a carrier vehicle even despite a loss of the payload due to a heavier re-entry winged booster as compared to conventional one-time upper stages, primarily due to elimination of the restricted impact areas.

The payload losses of the large space booster can be attenuated by the employment of the alternative RASS concept, which excludes direct RWB flying to the launch site.

The alternative RASS concept promises a payload gain up to 10% for the basic RWB configurations and up to 22% for the transformer-type re-entry winged boosters [5].

The autonomous flight mode has been proven preferable for the RWB ferry and flight tests compared with a conventional transportation on a super airlifter.

Acknowledgments

References

[1] Nesterov, V.E., Kuzin, A.I., Ivanov, V.L., Lozin, S.N., Lechov, P.A., Semenov, A.I., Panitchkin, N.G., Romashkin, A.M. Re-usable Space-Rocket System. Innovations on Development of Russian Means of Access to Outer Space. IAC-11-D2.4.4. *62nd International Astronautical Congress*, Cape Town, SA, 2011.

[2] Filatyev, A.S., Buzuluk, V.I., Yanova, O.V., Ryabukha, N.I., Petrov, A.N. Advanced Aviation Technology for Reusable Launch Vehicle Improvement. IAC-12-D2.5.7. *63rd International Astronautical Congress*, Naples, Italy, 2012.

[3] Filatyev, A.S., and Yanova O.V. ASTER Program Package for the Thorough Trajectory Optimization. *41st AIAA «Guidance, Navigation & Control» Conference*, 6-9 August 2001, Montreal, Canada, AIAA-2001-4391.

[4] Pontryagin, L.S., Boltyansky, V.G., Gamkrelidze, R.V., and Mischenko, E.F. *The Mathematical Theory of Optimal Processes*. Interscience Publishers, New York, 1962.

[5] Riabukha, N.N. Reusable rocket aircraft module and method of his return to the launch site. Patent RU 2442727, 20.02.2012. FIIP. *Invention bulletin, utility models*. № 5, 2012.

[6] Filatyev, A.S. Optimization of Branched Trajectories for Aerospace Transport Systems. ICAS-94-5.2.3. *19th ICAS Congress*, 18-23 September 1994, Anaheim CA, USA.

[7] Filatyev, A.S. "Paradoxes" of Optimal Solutions in Problems of Space Vehicle Injection and Reentry. *Acta Astronautica*, Vol.47, No.1, pp.11-18, 2000.

[8] Filatyev, A.S., and Yanova, O.V. Through optimization of branching injection trajectories by the Pontryagin maximum principle using stochastic models. *Acta Astronautica*, vol. 68, Issues 7-8, pp. 1042-1050, April-May 2011.

[9] Filatyev, A.S. Approximate Analytical Synthesis of the Optimal Control of Hypersonic Vehicles in Atmospheric Flight with Subcircular Velocities. *Uchenye Zapiski TsAGI*, v. 11, No.1, 2, 1980.

[10] Filatyev, A.S. Critical Reentry Conditions. ISTS 94-c-3. *19th International Symposium on Space Technology and Science*, Yokohama, Japan, 1994.

[11] Filatyev, A.S., and Yanova, O.V. Optimization of Space System Launching with Limitations on Fall Zones for Spent Components. ICAS-98-1.3.3. *21st ICAS Congress*, Melbourne, Victoria, Australia, 1998.

[12] Filatyev, A.S. Optimization of Spacecraft Ascent Using Aerodynamic Forces, IAF-92-0022. *43rd Congress of the International Aeronautical Federation*, August 28-Sept. 5, 1992, Washington, DC.

[13] Ving, Nguyen X. *Flight mechanics of high-performance aircraft*. Cambridge University Press, Great Britain, 1993.

[14] Bliss G.A. *Mathematics for Exterior Ballistics*. N. Y., 1944.

[15] Filatyev, A.S., Golikov, A.A., Shanygin, A.N., and Voityshen, V.S. The local distributed criteria method for multidisciplinary optimization of launcher parameters, *Acta Astronautica*, vol. 65, Issues 3-4, August-September 2009, pp. 584-590.

Copyright Statement